JOURNAL OF Materials CHEMISTRY

Growth conditions for wurtzite zinc oxide films in aqueous solutions

Satoshi Yamabi and Hiroaki Imai*

Department of Applied Chemistry, Keio University, 3-14-1 Hiyoshi, Kohoku-ku, Yokohama 223-8522, Japan. E-mail: hiroaki@applc.keio.ac.jp

Received 5th June 2002, Accepted 28th August 2002
First published as an Advance Article on the web 27th September 2002

A pH above 9.0 was essential for the formation of wurtzite zinc oxide (ZnO) in aqueous solution systems. The addition of complexing agents to decrease the deposition rate was required for the direct growth of ZnO on the surface of substrates through heterogeneous nucleation. The nucleation of the crystals was promoted by undercoats derived from zinc acetate. Wurtzite ZnO films consisting of hexagonal columns with diameters of 20–100 nm were successfully prepared on various substrates under suitable conditions.

1 Introduction

Recently, direct deposition techniques in aqueous solutions have been developed for the fabrication of various metal oxide films at low temperatures.[1–7] The principle of these processes is based on heterogeneous nucleation and subsequent crystal growth on a specific surface. Heterogeneous nucleation for film preparation is induced in supersaturated solutions at a relatively low degree of supersaturation. The conditions of the aqueous solutions are controllable by adjusting the concentration, temperature, and pH and selecting adequate quantities and kinds of additives, such as a complexing or chelating agents. Fabrication of thin films of silicon dioxide,[1] titanium dioxide,[2–4] tin oxide,[5] and magnetite[6,7] has already been achieved in aqueous solutions at low temperatures using these methods. In the near future, these low-energy and less hazardous techniques will become more attractive as a possible alternatives for film preparation because of their advantages over conventional dry and wet processes.

Wurtzite zinc oxide (ZnO) is of interest in many applications for transparent conductive coatings,[8] electrodes for dye-sensitized solar cells,[9] gas sensors,[10] and luminescent materials[11] due to its useful characteristics. ZnO thin films have been prepared by various dry processes such as chemical vapor deposition (CVD),[12] radio frequency magnetron sputtering,[13,14] and molecular beam epitaxy (MBE).[15] Wet processes, including the sol–gel method,[16,17] spray pyrolysis,[18] and electrodeposition,[19,20] were also valuable for the preparation of the oxide film. There are many previous studies for ZnO films using direct deposition techniques in aqueous solutions. Table 1 lists the earlier studies on the preparation of ZnO thin films in aqueous solution systems using zinc salts. The formation of wurtzite ZnO was reported using various systems at near room temperatures. Izaki *et al.*[21,22] prepared ZnO films by chemical reaction with dimethylamineborane (DMAB). Highly oriented crystalline films were grown directly on a substrate in aqueous solutions containing urea with the flowing liquid film method.[23] O'Brien *et al.*[24] obtained crystalline films in alkaline aqueous solutions containing ethane-1,2-diamine (en) as a chelating agent. Thin films consisting of well-aligned ZnO microrods were formed by the thermal decomposition of an amino complex formed with Zn^{2+} and methenamine.[25,26] However, the essence of the formation of a wurtzite ZnO phase in aqueous solution systems is not clear because the conditions adopted in these studies were highly diverse. Moreover, zinc hydroxide[27] and zinc fluoride hydroxide[28] films were also deposited in aqueous solutions under similar conditions, as shown in Table 1. In the present work, therefore, we investigated the essential conditions for the growth of wurtzite ZnO films in aqueous solutions using zinc sulfate and various kinds of ammonium salts as the complexing agent. The effects of pH and complexing agent are discussed in this paper. The surface conditions for heterogeneous nucleation of ZnO are also described, and suitable undercoats for the preparation of wurtzite ZnO films are proposed.

2 Experimental

Stock solutions containing 0.02 M zinc sulfate heptahydrate ($ZnSO_4 \cdot 7H_2O$; Kanto Chemical) and a certain amount of complexing agent were prepared using purified water. Ammonium fluoride (NH_4F), ammonium chloride (NH_4Cl), ammonium nitrate (NH_4NO_3), and ammonium sulfate ($(NH_4)_2SO_4$) (Junsei Chemical) were each used as the complexing agent. The molar ratio ($R = NH_4^+/Zn^{2+}$) for NH_4F was adjusted in the range of 20–50. When $(NH_4)_2SO_4$ was added into the solutions, equimolar sodium sulfate (Na_2SO_4; Junsei Chemical) was also dissolved in order to equalize the quantity of SO_4^{2-} to that of the anions in the other systems.

Precursor solutions with a Zn concentration of 0.01 M were prepared from the stock solutions. The pH value of the precursor solutions was adjusted to be in the range between 3.00 and 13.00 by adding NaOH aqueous solutions (1 or 5 M). Substrates were immersed into the precursor solutions and maintained at 60 °C. After 1–10 days, the substrates were withdrawn from the solutions, rinsed with purified water, and

Table 1 Earlier works for synthesis of ZnO thin films with aqueous solutions

As-deposited	Zinc source	Additive	pH	*T*/°C	Annealing/°C	Ref.
ZnO	$Zn(NO_3)_2$	DMAB	6.2	50	None	21,22
ZnO	$ZnCl_2$	Urea	8.0	70	None	23
ZnO	$Zn(CH_3COO)_2$	En	9–12	50	None	24
ZnO	$Zn(NO_3)_2$	Methenamine	—	90–95	None	25,26
$Zn(OH)_2$	$ZnCl_2$	NH_4F	7.5–8.5	25	200	27
ZnF(OH)	$ZnCl_2$	NH_4F	7.0–8.5	25	300	28

dried at room temperature. Glass slides, silicon wafers, poly(ethylene terephthalate) (PET) sheets, and conductive glass plates coated with fluorine-doped tin oxide (FTO) were used as a substrate. Undercoats derived from zinc acetate were utilized for the promotion of heterogeneous nucleation. Underlying thin layers with a thickness of $\sim$100 nm were fabricated on glass slides and PET sheets by spinning of 2-methoxyethanol solution containing zinc acetate dihydrate ($Zn(CH_3COO)_2{\cdot}2H_2O$; Kanto Chemical) and monoethanolamine.[16] The obtained thin layers were dried at 60 °C for 24 h.

X-Ray diffractometry (XRD) was performed with a Rigaku RAD-C using Cu-Kα radiation by the $2\theta/\theta$ scanning mode. Macroscopic and microscopic morphologies were observed with a field emission scanning electron microscope (FESEM; Hitachi S-4700). X-Ray photoelectron spectroscopy (XPS) was carried out with a JEOL JPS-9000MC using Mg-Kα radiation to analyze the surface contamination.

3 Results

3.1 Phase diagram

Fig. 1 shows a diagram of the solid phases deposited in aqueous solutions containing 0.01 M $ZnSO_4$ and various amounts of NH_4F as the complexing agent. The crystal phase and the mode of deposition (*via* heterogeneous nucleation on the surface of the substrates or homogeneous nucleation in the bulk of the solutions) were influenced by the molar ratio of the complexing agent to the zinc source (R) and the pH of the solutions. In particular, the crystal phase was found to be mainly determined by the pH value of the solutions. The aqueous solutions in region I (pH 3.0–6.0) were transparent for 10 days without deposition on the substrate surfaces and precipitation in the bulk solutions. Deposition on the surface of substrates or precipitates consisting of orthorhombic zinc fluoride hydroxide (ZnF(OH)) was observed in region II (pH 6.0–9.0). Hexagonal ZnO crystal (wurtzite structure) was deposited on the surface and precipitated in region III (pH 9.0–13.0). The mode of the deposition was influenced by the molar ratio of the complexing agent. Deposition on the surface of the substrates through heterogeneous nucleation was dominant in regions II and III. At low R conditions ($\sim$20), however, precipitation rapidly occurred *via* homogeneous nucleation in the bulk without heterogeneous nucleation. A small amount of unidentified crystals and ε-$Zn(OH)_2$ was contained in the precipitates in regions II and III, respectively. No solid phases were produced with relatively high R values (30–50) at pH 8.5–11.5 and above 12.5. Generally, the presence of complexing agents reduces the deposition rate of the solid phases with the complexation of soluble species. Thus, an increase in R suppressed the homogeneous nucleation in the bulk and promoted the heterogeneous nucleation on the surface. The soluble species

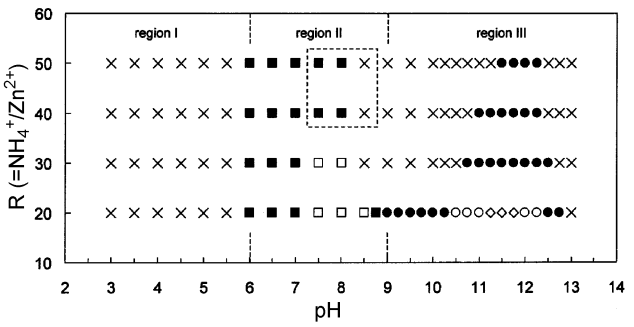

Fig. 1 Diagram of the crystal phases deposited in the aqueous solutions and the mode of deposition. Experiments were carried out with NH_4F as the complexing agent. Symbols: ×, no deposition and precipitation; ■, deposition of ZnF(OH); □, precipitation of ZnF(OH) with a few unidentified crystals; ●, deposition of ZnO; ○, precipitation of ZnO; ◇, precipitation of ZnO with a little ε-$Zn(OH)_2$.

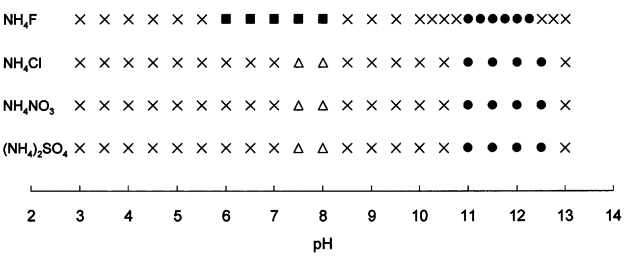

Fig. 2 Effects of the counter anions of the complexing agents on the crystal phase of the products and the mode of deposition. NH_4F, NH_4Cl, NH_4NO_3 and $(NH_4)_2SO_4$ were used as the complexing agent at $R = 40$. Symbols: ×, no deposition and precipitation; ■, deposition of ZnF(OH); ●, deposition of ZnO; △, precipitation of hydroxide.

were apparently stabilized with a great amount of the complexing agent ($R > 50$).

3.2 Effects of complexing agents

Fig. 2 shows the effects of the counter anions of different ammonium salts on the crystal phase of the deposits. The solutions were transparent and no solid phases were produced for 10 days in region I when NH_4Cl, NH_4NO_3, and $(NH_4)_2SO_4$ were used as the complexing agent at $R = 40$. In region III, wurtzite ZnO crystals were directly grown on the surface of the substrates at pH 11.0–12.5. This behavior for the solutions in regions I and III was almost the same as that for NH_4F. In region II, however, the solutions were apparently stable at pH 6.0–7.0 and turbid with precipitation at pH 7.5–8.0. The precipitates produced with Cl^-, NO_3^-, and SO_4^{2-} were unidentified crystals although ZnF(OH) was obtained with F^- in region II. The unknown crystalline precipitates did not contain chlorine, nitrogen, or sulfur and were transformed into wurtzite ZnO by calcination at 500 °C. We have concluded that these unknown phases are various kinds of zinc hydroxides. In this pH region, therefore, zinc hydroxides were precipitated in the solutions. ZnF(OH) was produced with NH_4F because the coordination of F^- to Zn^{2+} cations was greater than that of the other counter anions. Deposition on the surface *via* heterogeneous nucleation mainly occurred with F^- although precipitates *via* homogeneous nucleation were obtained with the other anions. This behavior is explainable by a reduction in the deposition rate due to the coordination of F^- to Zn^{2+} cations. Fig. 3 indicates that deposition on the surface *via* heterogeneous nucleation was also achieved with increasing R with NH_4Cl as the complexing agent.

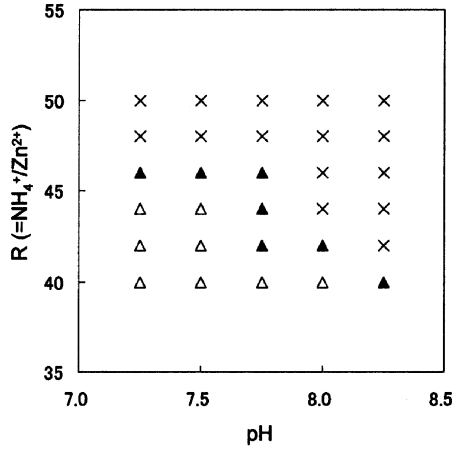

Fig. 3 Diagram of the crystal phases deposited in aqueous solutions and the mode of deposition. Experiments were carried out with NH_4Cl as the complexing agent in the condition area enclosed by the dashed square in Fig. 1. Symbols: ×, no deposition and precipitation; ▲, deposition of hydroxide; △, precipitation of hydroxide.

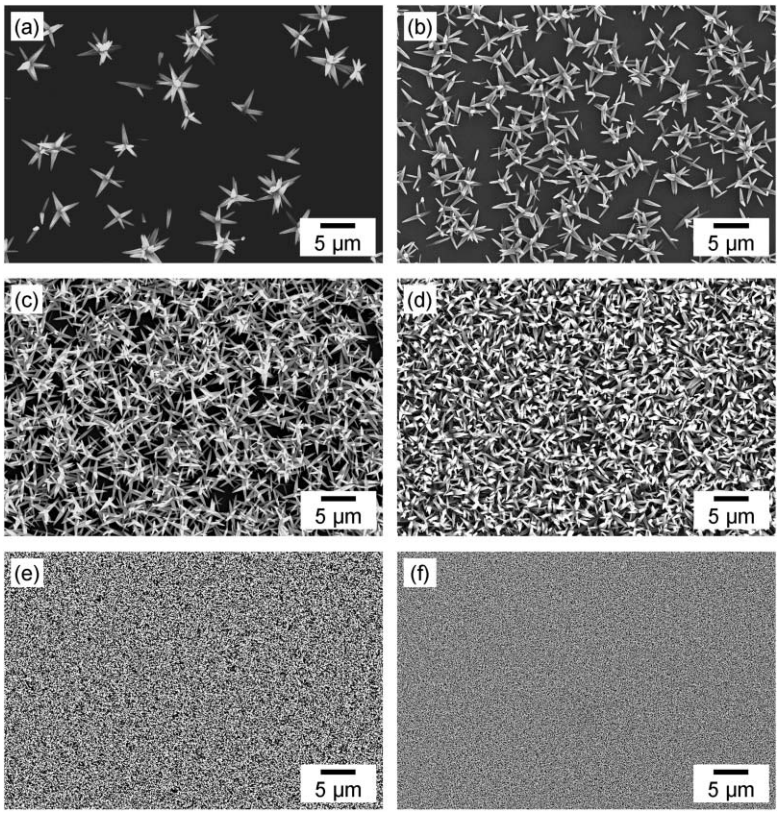

Fig. 4 FESEM micrographs for as-deposited ZnO crystals on a glass slide (a), silicon wafer (b), PET (c), FTO (d), amorphous undercoat (e), and crystalline undercoat (f). The crystals were deposited in aqueous solutions with NH_4Cl at pH 11.00 and $R = 30$.

3.3 Effects of the surface of substrates

Fig. 4 shows the FESEM micrographs of the ZnO crystals deposited on various substrates having diverse characteristics. Precursor solutions containing NH_4Cl at pH 11.00 and $R = 30$ were used for the deposition. Clusters of spindle-shaped hexagonal crystallites with diameters of 0.5–1.0 μm were scattered over the surface of a glass slide and a silicon wafer. A larger number of the clusters were formed on a PET sheet and an FTO-coated glass plate. Densely packed columnar crystals formed a film of $\sim$2 μm thickness on the surface of undercoats derived from zinc acetate regardless of the substrate characteristics. The underlying thin layers were composed of an amorphous phase and a small amount of zinc monoacetate. The undercoats were transformed into wurtzite ZnO by calcination at 500 °C. As exhibited in Fig. 5, a great number of hexagonal columns with diameters of 20–100 nm were deposited perpendicularly to the surface of the crystalline undercoats. Fig. 6 shows the XRD profiles for the deposited film and the underlying crystalline layer. Because the intensity of the peak assigned to the (002) plane of wurtzite ZnO was markedly large and the diffraction peaks of other crystal planes disappeared or were very weak, the (002) planes were strongly oriented perpendicularly to the substrate surface. Thus, the columnar rods composing the films were formed through elongation along the *c* axis. The degree of the *c* axis orientation of wurtzite ZnO films was remarkable high on the underlying crystalline layers.

4 Discussion

4.1 Conditions for the formation of wurtzite ZnO

In this work, we found that the crystal phase of the deposits was mainly determined by the pH of the aqueous solutions. Fig. 7 shows the phase stability diagrams for the $ZnO–H_2O$ and $Zn(OH)_2–H_2O$ systems at 25 °C. The dashed lines denote the thermodynamic equilibria between the Zn(II) soluble species and the solid phases. The boundaries were calculated on the basis of the equilibria and thermodynamic data shown in Tables 2 and 3, respectively.[29,30] The solid lines represent the total concentration of the soluble species as a function of pH, *i.e.*, the solubility of the solid phases. In the diagrams, the soluble species are stable below pH $\sim$7 at a Zn concentration of 0.01 M. This fact is consistent with our results showing that

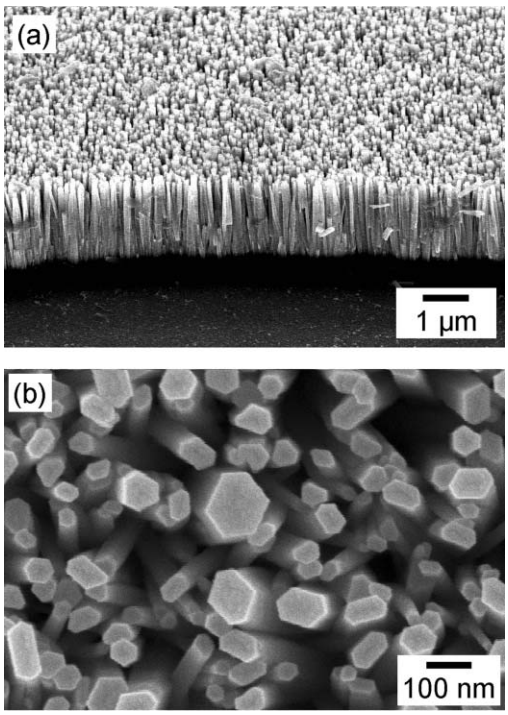

Fig. 5 FESEM micrographs for a ZnO film on a crystalline undercoat shown in Fig. 4(f). The tilt angles for the FESEM observation are 45° (a) and 0° (b).

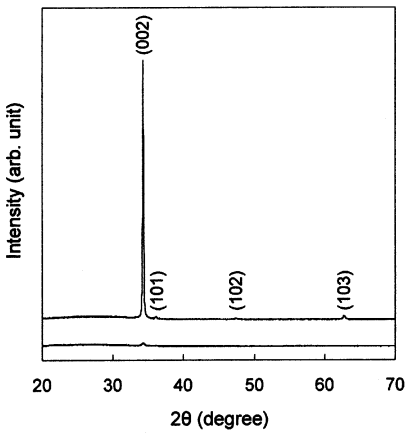

Fig. 6 XRD profiles for a crystalline undercoat (lower) and a ZnO film formed on a crystalline undercoat (upper).

the aqueous solutions were stable in region I. These diagrams indicate that the solubility of ZnO is almost the same as that of $Zn(OH)_2$. Thus, both $Zn(OH)_2$ and ZnO are thermodynamically stable over a pH range of 7 to 14 at a 0.01 M Zn concentration. In the present study, however, $Zn(OH)_2$ was predominantly formed at pH 6.0–9.0 (region II), while wurtzite ZnO was mainly obtained at pH 9.0–13.0 (region III).

In aqueous solutions at pH >9, as shown in Fig. 7, Zn(II) soluble species in the form of hydroxyl complexes such as $Zn(OH)_2(aq)$ and $Zn(OH)_4^{2-}$ increase.[29,30] It is expected that the equilibrium in eqn. (1) moves to the right because the chemical potential of OH^- in a system increases with increasing pH.

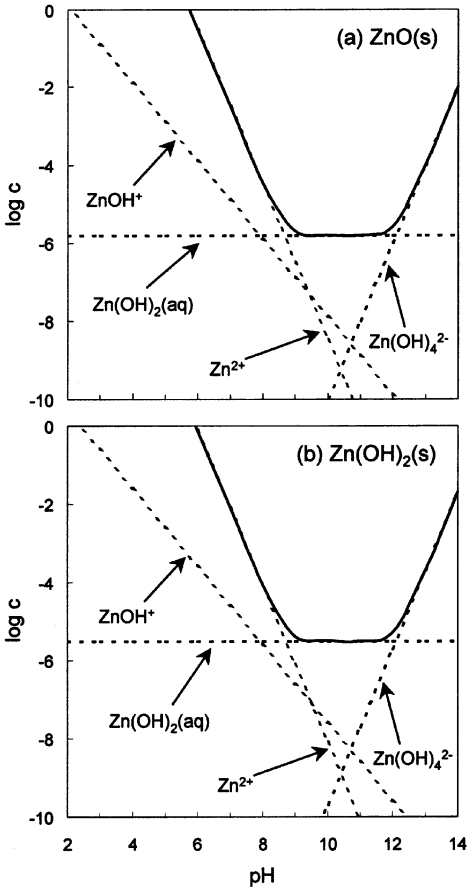

Fig. 7 Phase stability diagrams for the ZnO(s)–H_2O (a) and $Zn(OH)_2$(s)–H_2O (b) systems at 25 °C as a function of pH. An equilibrium between $Zn(OH)_3^-$ and the solid phases is out of the range.

Table 2 Thermodynamic equilibria for ZnO(s)–H_2O and $Zn(OH)_2$(s)–H_2O systems

ZnO(s)–H_2O	$Zn(OH)_2$(s)–H_2O
$Zn^{2+} + H_2O \leftrightarrow ZnO(s) + 2H^+$	$Zn^{2+} + 2H_2O \leftrightarrow Zn(OH)_2(s) + 2H^+$
$ZnOH^+ \leftrightarrow ZnO(s) + H^+$	$ZnOH^+ + H_2O \leftrightarrow Zn(OH)_2(s) + H^+$
$Zn(OH)_2(aq) \leftrightarrow ZnO(s) + H_2O$	$Zn(OH)_2(aq) \leftrightarrow Zn(OH)_2(s)$
$Zn(OH)_3^- + H^+ \leftrightarrow ZnO(s) + 2H_2O$	$Zn(OH)_3^- + H^+ \leftrightarrow Zn(OH)_2(s) + H_2O$
$Zn(OH)_4^{2-} + 2H^+ \leftrightarrow ZnO(s) + 3H_2O$	$Zn(OH)_4^{2-} + 2H^+ \leftrightarrow Zn(OH)_2(s) + 2H_2O$

Table 3 Thermodynamic data for ZnO(s), $Zn(OH)_2$(s) and soluble species at 298 K[29]

Species	$\Delta_f G°$/kJ mol^{-1}	Species	$\Delta_f G°$/kJ mol^{-1}
ZnO(s)	−318.3	Zn^{2+}(aq)	−147.0
$Zn(OH)_2$(s)	−553.6	$ZnOH^+$(aq)	−330.1
		$Zn(OH)_2$(aq)	−522.3
H^+(aq)	0	$Zn(OH)_3^-$(aq)	−694.3
H_2O(l)	−237.2	$Zn(OH)_4^{2-}$(aq)	−858.7

$$OH^- + OH^- \leftrightarrow O^{2-} + H_2O \quad (1)$$

Thus, when these hydroxyl complexes transform into the solid phases, Zn–O–Zn bonds are constructed due to the above-mentioned dehydration reaction in eqn. (1) as

$$Zn(OH)_n^{2-n} + Zn(OH)_n^{2-n} \leftrightarrow Zn_2O(OH)_{2n-2}^{4-2n} + H_2O \quad (2)$$

where $n = 2$ or 4. The crystal structure of ZnO was gradually constructed by dehydration between OH^- on the surface of the growing crystals and the OH^- ligands of the hydroxyl complexes. In this system, therefore, the formation of wurtzite ZnO at pH >9.0 occurs because of an increase in the concentration of the precursors and the chemical potential of OH^- with increasing pH. Li *et al.*[31] explained the growth mechanism of wurtzite ZnO with the hypothesis that $Zn(OH)_4^{2-}$ as a growth unit was incorporated into the crystal lattice by a dehydration reaction, although they did not describe the effect pH had on the growth conditions of ZnO. Hence, this hypothesis supports our suggestion about the formation of ZnO in aqueous media at pH >9.0.

Soluble ionic forms are Zn^{2+} and $ZnOH^+$ under acidic conditions of pH $< \sim 6.0$.[29,30] With increasing OH^- in the aqueous solution, the precipitation of $Zn(OH)_2$ occurs under neutral and moderately basic pH conditions as

$$Zn^{2+} + 2OH^- \leftrightarrow Zn(OH)_2 \quad (3)$$

However, ZnF(OH) was produced in the aqueous solutions under neutral conditions with NH_4F. Saito *et al.*[28] have already reported that ZnF(OH) was obtained with NH_4F at pH 7.0–8.5. The formation of fluoride hydroxide is ascribed to the coordination of the most electronegative anions to Zn^{2+} cations. Heterogeneous nucleation of ZnF(OH) occurs on the surface with a lower deposition rate in region II since Zn^{2+} cations form ZnF^+ complexes in the presence of F^-. According to the literature,[27,28] $Zn(OH)_2$ is precipitated at lower contents of NH_4F. This result suggests that $Zn(OH)_2$ is in a stable state under neutral and moderately basic conditions (region II) without F^-. As shown in Fig. 1, $Zn(OH)_2$ crystals were also produced at a small R value in aqueous solutions even at pH >9.0. Hydroxide is assumed to be formed as a metastable impurity phase due to rapid precipitation.

As shown in Fig. 2, the crystal phase of the products was not affected by the kinds of complexing agents, except for the formation of ZnF(OH) in region II. With the partial charge model (PCM),[32,33] we previously explained the effect of coexisting anions on the crystal phase and morphology of TiO_2 thin films with rutile and anatase structures.[4] The PCM suggests that F^-, Cl^-, NO_3^-, and SO_4^{2-} anions can coordinate with Zn^{2+} cations in the pH range of −2.90–7.78, 3.13–8.12, −6.81–1.71, and −4.64–9.41, respectively. Because the above-mentioned anions cannot coordinate to Zn^{2+} cations in region III, the formation of the ZnO crystal was not affected by the coexisting anions in aqueous solutions. In fact, fluorine, chlorine, nitrogen, and sulfur were not detectable on the surface of the as-deposited ZnO crystals by XPS analysis.

As listed in Table 1, there have been many studies on the synthesis of wurtzite ZnO in aqueous solutions.[21–26] O'Brien *et al.*[24] obtained crystals in aqueous solutions at pH >9.5. Their results almost agree with our conclusion; however, they used ethane-1,2-diamine as the chelating agent. In other studies, the pH values of the precursor solutions were below 8.0. However, when DMAB,[21,22] urea,[23] and methenamine[25,26] are contained in the precursor solutions, they increase the pH in the systems by decomposition during the process. Thus, we assume that the pH values in the solutions locally increased to >9.0 at the growing interface of the crystals.

4.2 Conditions for heterogeneous nucleation

Deposition of the crystal phases on the surface of the substrates was commonly observed in regions II and III with relatively high R values except at pH 8.5–10.5 ($R = 30$) and 8.5–11.5 ($R = 50$). In these restricted regions, deposition on the surface was observed with $R = \sim 20$, and no deposits or precipitates were produced with increasing the R. Generally, deposition on the surface through heterogeneous nucleation occurs with a low deposition rate in supersaturated solutions at a low degree of supersaturation. In our systems, the solubility, as a function of the pH, and the stabilization of the soluble species, *via* complexation, are important for the control of the deposition rate. According to the phase diagrams shown in Fig. 7, the pH ranges 6.0–9.0 and 11.5–13.0 are a transition condition in which the solubility steeply varies with the pH. Fundamentally, deposition on the substrates was achieved in these ranges with a large amount of ammonium salts for complexation.

Zn^{2+} cations form ammine complexes of $Zn(NH_3)_n^{2+}$ (n = 1–4) with NH_3(aq) in moderately basic media[28] as

$$Zn^{2+} + nNH_3(aq) \leftrightarrow Zn(NH_3)_n^{2+} \quad (4)$$

The concentration of ammine complexes increases with an increase of the ammonium salts. The degree of supersaturation for the solid phases decreased with increasing R because the equilibrium in eqn. (4) moves to the right. Thus, solutions of pH 8.5–11.5 were stable with a large amount of the complexing agents. In this region, deposition was observed with a relatively small amount of the ammonium salts ($R = \sim 20$).

In the pH region above 10.5, because the total concentration of NH_3 in the aqueous solution becomes lower due to a decrease in the NH_3 solubility in water,[29] the equilibrium in eqn. (4) moves to the left. Therefore, deposition and precipitation were observed. Because the solubility of Zn(II) solid phases increases above pH 11.5, stable solutions were obtained in this region.

Deposition of ZnF(OH) was observed with NH_4F at pH levels around 6.0–8.0 although precipitates of hydroxides were obtained with the other ammonium salts. Because the hydrolysis and condensation rates were dramatically reduced by the complexation of Zn^{2+} cations with F^-, heterogeneous nucleation of fluoride hydroxide was achieved in the solutions. The hydroxides were deposited on the substrates even with NH_4Cl at high R values (above 40) as shown in Fig. 3. In this case, the heterogeneous nucleation with the low deposition rate was ascribed to a decrease in the free Zn^{2+} concentration by its complexation with ammonium.

4.3 Promotion of nucleation by undercoats

As shown in Fig. 4, the density of the deposited ZnO crystals was remarkably affected by the surface of the substrates. The density is attributed to the number of nucleation sites on the surface. However, no relationships between the number of nucleus forming and the property of the surfaces, such as wettability and conductivity, were recognized. However, the undercoats derived from zinc acetate obviously promoted nuclei formation. This promotion of heterogeneous nucleation is ascribed to the high affinity of the nuclei of wurtzite ZnO for the surface. Various activation processes for the surface have also been reported for the promotion of nucleation with other techniques for the formation of ZnO films.[21,22,34,35] These facts indicate that the nucleation of wurtzite ZnO is generally difficult. The preparation of undercoats is a simple and convenient route for the promotion of nucleation. This method is applicable to various polymer sheets because heat treatment is not generally required for the preparation.

The wurtzite ZnO films grown on crystalline undercoats had the preferential orientation of the c axis, perpendicular to the substrate, as shown in Fig. 5. FESEM analysis revealed that the ZnO film consisted of nanosized crystallites with hexagonal columns arranged vertically to the substrate surface. The c axis is the preferential growth direction due to the instability of the polar (002) plane.[36,37] Although crystal growth in any direction occurs at the nuclei on the surface, the preferential direction of the c axis would be maintained as the crystal growth proceeds. This markedly preferred orientation is ascribed to the well-ordered arrangement of the columnar crystallites.

5 Conclusions

The essential conditions for the preparation of wurtzite ZnO crystals in aqueous solutions at near ambient conditions were clarified using various kinds of ammonium salts as the complexing agent. The crystal phases were fundamentally determined by the pH of the aqueous solution systems. Wurtzite ZnO was produced in a basic region of pH from 9.0 to 13.0. Deposition on the surface of the substrates *via* heterogeneous nucleation was achieved with a decrease in the deposition rate by changing the pH and the concentration of the complexing agents. The nucleation of the crystals was promoted by means of underlying thin layers derived from zinc acetate. Therefore, thick films of wurtzite ZnO consisting of columnar rods with diameters of 20–100 nm were successfully produced in aqueous solutions at 60 °C. This technique is applicable for the preparation and patterning of functional ZnO films on various kinds of substrates at low temperatures.

Acknowledgement

We thank Mr. E. Hosono, Ceramic Science Laboratory, Keio University, for preparation of an undercoat.

References

1 H. Nagayama, H. Honda and H. Kawahara, *J. Electrochem. Soc.*, 1988, **135**, 2013.
2 S. Deki, Y. Aoi, O. Hiroi and A. Kajinami, *Chem. Lett.*, 1996, 433.
3 S. Yamabi and H. Imai, *Chem. Lett.*, 2001, 220.
4 S. Yamabi and H. Imai, *Chem. Mater.*, 2002, **14**, 609.
5 K. Tsukuma, T. Akiyama and H. Imai, *J. Non-Cryst. Solids*, 1997, **210**, 48.
6 M. Abe and Y. Tamaura, *Jpn. J. Appl. Phys.*, 1983, **22**, L511.
7 M. Izaki and O. Shinohara, *Adv. Mater.*, 2001, **13**, 142.

8 T. Minami, *J. Vac. Sci. Technol. A*, 1999, **17**, 1765.
9 H. Rensmo, K. Keis, H. Lindström, S. Södergren, A. Solbrand, A. Hagfeldt, S. E. Lindquist, L. N. Wang and M. Muhammed, *J. Phys. Chem. B*, 1997, **101**, 2598.
10 K. S. Weißenrieder and J. Müller, *Thin Solid Films*, 1997, **300**, 30.
11 S. Sakahara, M. Ishida and M. A. Anderson, *J. Phys. Chem. B*, 1998, **102**, 10169.
12 H. Sato, T. Minami, T. Miyata, S. Tanaka and M. Ishii, *Thin Solid Films*, 1994, **246**, 65.
13 K. H. Yoon, J. W. Choi and D. H. Lee, *Thin Solid Films*, 1997, **302**, 116.
14 S. Takada, *J. Appl. Phys.*, 1993, **73**, 4739.
15 Y. Chen, D. M. Bagnall, Z. Zhu, T. Sekiuchi, K. Park, K. Hiraga, T. Yao, S. Koyama, M. Y. Shen and T. Goto, *J. Cryst. Growth*, 1997, **181**, 165.
16 M. Ohyama, H. Kozuka and T. Yoko, *Thin Solid Films*, 1997, **306**, 78.
17 A. E. Jimenez-Gonzalez, J. A. S. Urueta and R. Suarez-Parra, *J. Cryst. Growth*, 1998, **192**, 430.
18 D. J. Goyal, C. Agashe, M. G. Takwale, B. R. Marathe and V. G. Bhide, *J. Mater. Sci.*, 1992, **27**, 4705.
19 S. Peulon and D. Lincot, *Adv. Mater.*, 1996, **8**, 166.
20 M. Izaki and T. Ohmi, *Appl. Phys. Lett.*, 1996, **68**, 2439.
21 M. Izaki and T. Ohmi, *J. Electrochem. Soc.*, 1997, **144**, L3.
22 M. Izaki and J. Katayama, *J. Electrochem. Soc.*, 2000, **147**, 210.
23 K. Ito and K. Nakamura, *Thin Solid Films*, 1996, **286**, 35.
24 P. O'Brien, T. Saeed and J. Knowles, *J. Mater. Chem.*, 1996, **6**, 1135.
25 L. Vayssieres, K. Keis, S. T. Lindquist and A. Hagfeldt, *J. Phys. Chem. B*, 2001, **105**, 3350.
26 L. Vayssieres, K. Keis, A. Hagfeldt and S. T. Lindquist, *Chem. Mater.*, 2001, **13**, 4395.
27 D. Raviendra and J. K. Sharma, *J. Appl. Phys.*, 1985, **58**, 838.
28 N. Saito, H. Haneda, W. S. Seo and K. Koumoto, *Langmuir*, 2001, **17**, 1461.
29 W. Stumm and J. J. Morgan, *Aquatic Chemistry*, Wiley-Interscience, New York, 1995, p. 1002.
30 R. A. Reichle, K. G. McCurdy and L. G. Hepler, *Can. J. Chem.*, 1975, **53**, 3841.
31 W. J. Li, E. W. Shi, W. Z. Zhong and Z. W. Yin, *J. Cryst. Growth*, 1999, **203**, 186.
32 J. Livage, M. Henry and C. Sanchez, *Prog. Solid State Chem.*, 1988, **18**, 259.
33 M. Henry, J. P. Jolivet and J. Livage, *Struct. Bonding*, 1992, **77**, 153.
34 B. O'Regan, V. Sklover and M. Grätzel, *J. Electrochem. Soc.*, 2001, **148**, C498.
35 N. Saito, H. Haneda, T. Sekiguchi, N. Ohashi, I. Sakaguchi and K. Koumoto, *Adv. Mater.*, 2002, **14**, 418.
36 R. A. Laudise and A. A. Ballman, *J. Phys. Chem.*, 1960, **64**, 688.
37 R. A. Laudise, E. D. Kolb and A. J. Caporaso, *J. Am. Ceram. Soc.*, 1964, **47**, 9.